

# Influence of the Burnout in Vitiators on Ignition Limits in Scramjet Combustors

Tobias Sander,\* Anatoliy Lyubar,\* and Thomas Sattelmayer†  
*Technical University of Munich, 85747 Garching, Germany*

and  
Eduard A. Shafranovsky‡  
*Russian Academy of Sciences, 119991, Moscow, Russia*

The influence of radicals emitted by a vitiator into a model of a hydrogen-fueled scramjet combustor was investigated. The effect of the preheater combustion was analyzed by varying between a flame mode with high radical formation and a flame mode in which the concentration of the OH radicals was reduced below the detection limit of the optical system. The ignition performances of two fuel injectors were compared to estimate the influence of radicals and water molecules from the preheater on the different types of flame stabilization. The shock wave system, the hydrogen air mixing, and the flame stabilization were studied with optical methods and computational fluid dynamics. It was observed that the two injectors react differently with increasing radical content in the incoming air. The injector with high total pressure loss is insensitive to the burnout in the preheater, whereas the injector that achieves low losses is considerably influenced by the quality of the air preheating. Thus, the cases of higher technical interest with a low pressure loss are more difficult to investigate using test rigs with vitiated air. A technical solution for improving the vitiator burnout, which allows the use of vitiators even in these critical cases, is presented.

## I. Introduction

INCREASING the payload is the most important factor for the economic design of hypersonic transportation systems. Because the weight of the oxidizer dominates the takeoff weight of rocket-based propulsion systems,<sup>1</sup> airbreathing engines offer a promising alternative.

Gas turbines, ramjets and scramjets are the components of future airbreathing propulsion systems. Below flight Mach number 2.5, gas turbines offer the best efficiency, whereas ramjet engines cover the range between 2.5 and 6. Beyond 6, however, the high static temperature resulting from the deceleration to subsonic speed leads to the dissociation of the air and to thermal problems in the ramjet engine. Under these conditions the scramjet engine, in which the flow remains supersonic, has the best performance.

The key to scramjet combustion is the proper design of the fuel injector, which must reconcile the opposing goals of low pressure loss, intense mixing, and high flame stability. To simulate the inlet conditions of a scramjet combustion chamber at supersonic flight, high-temperature test air is required. Test setups for scramjet injectors that use a hydrogen-powered vitiator for air preheating are widely used in research due to its inherent simplicity and low cost. Yet, it is widely known in the combustion community that results from measurements using vitiated air must be carefully interpreted because an influence of the preheater combustion products on the performance of the scramjet cannot be excluded. OH radicals, for example, have a strong accelerating influence on the ignition of a hydrogen–air mixture.<sup>2–4</sup> The required judgement is very difficult to make because there is no consensus on the quantitative relevance of vitiator effects in cases of technical interest.

It is the goal of the paper to specify which configurations can be investigated successfully with simple test rigs using vitiated air. Furthermore, the paper provides a vitiator design with perfect burnout and low radical concentrations at the vitiator exit. For this purpose, numerical and experimental investigations were carried out with the model of a scramjet combustion chamber, which was used earlier by Grünig.<sup>5</sup> The important disadvantage of his experimental setup was the observed influence of the preheater radical emissions on the ignition and reaction characteristics of the combustion chamber. Numerical simulation of the combustion processes in the chamber indicated that the reaction is initiated in the subsonic wake behind the strut, where the static temperature exceeds ignition limit but extinguishes downstream of the wake. However, stable combustion and burnout were observed in the experiment.<sup>6,7</sup> These inconsistent results initiated the current work.

In a first step, several possible reasons for the emission of radicals by the preheater are discussed, and laser-induced fluorescence (LIF) measurements, which were carried out at the exit of the Laval nozzle, are presented. These revealed considerable fluorescence signals, indicating an incomplete burnout in the preheater, which was a diffusion-type combustor. Incomplete burnout is a common feature of vitiators with diffusive burning and not specific to the vitiator employed in this study.

After the results of the LIF measurements had indicated that a diffusion-flame-type vitiator was unsuitable for the investigation of self-ignition, the combustion process was improved. The novel vitiator design is described. Complete burnout upstream of the scramjet is achieved by changing the reaction mode in the preheater from a non-premixed (diffusion) to a partially premixed flame. The required hardware changes are illustrated. An additional vortex generator with a second hydrogen injector upstream of the preheater is required for this purpose. Fuel switching allows then a variable selection of the radical content at the vitiator exit.

A general problem of scramjets is the low residence time in the combustor. To obtain a complete burnout within the chamber, an adequate mixing of the fuel and oxidizer must be obtained, and in addition, self-ignition of the fuel must be achieved right after the injection. Both tasks must be accomplished by a proper injector design. On the one hand, the injector must generate sufficient turbulence and a shock wave system that increases static temperature and

Received 24 April 2002; revision received 12 March 2003; accepted for publication 18 July 2003. Copyright © 2003 by the American Institute of Aeronautics and Astronautics, Inc. All rights reserved. Copies of this paper may be made for personal or internal use, on condition that the copier pay the \$10.00 per-copy fee to the Copyright Clearance Center, Inc., 222 Rosewood Drive, Danvers, MA 01923; include the code 0001-1452/04 \$10.00 in correspondence with the CCC.

\*Research Scientist, Lehrstuhl für Thermodynamik, Fakultät für Maschinenwesen.

†Professor, Lehrstuhl für Thermodynamik, Fakultät für Maschinenwesen.

‡Professor, Semenov Institute of Chemical Physics, Kosyguin Str. 4.

pressure. On the other hand, turbulence and the shock wave system both lead to a loss of total pressure that reduces the efficiency of the propulsion system.

In the studies of Grünig<sup>7</sup> and Grünig et al.,<sup>8</sup> a pylon injector was designed with the goal of optimizing the mixture preparation and the reaction. This rather massive injector produces a strong shock wave system in combination with secondary vortices and leads to an intense reaction. Because of the high pressure losses caused by the pylon, it is questionable whether this design is technically viable. However, the geometry can provide reference data for an injector with very robust flame stabilization. For comparison, a slender strut injector was designed in the framework of the current study. This design provides less rigorous flame stabilization but with lower pressure loss. By the comparison of the results of the two designs, the effects of the inflowing radicals and the water vapor content on the ignition process will be illustrated.

## II. Experimental Setup

### A. Model Scramjet Combustor

The model scramjet combustor is shown in Fig. 1. The filtered test air, which is supplied with pressures up to 13 bar, is mixed with oxygen to compensate for the oxygen loss in the hydrogen preheater. The total temperature in the preheater can be increased up to 1400 K and is measured with an accuracy of 3%. The maximum mass flow through the channel was  $300 \text{ g/s} \pm 3\%$  during experiments. The preheated flow is expanded subsequently in a Laval nozzle to a Mach number of 2.1 and enters the combustion chamber.

### B. Preheater

The hydrogen required for the preheating of the test air ignites in the preheater immediately after its addition to the main flow, and a diffusive flame is stabilized by flame holders (Fig. 2). The residence time of the gas in the preheater is rather short to obtain a perfect mixture as its length is only 380 mm. This limits the burnout that can be achieved before the gases leave the preheater. To obtain a higher burnout with low radical content in the exhaust, a vortex generator was installed 700 mm upstream of the preheater (Fig. 1). Half of the fuel is injected at the vortex generator, and half of the fuel is added at the original downstream injector to obtain partially premixed combustion. In this mode, the flame holder acts as stabilization device for the piloted partially premixed flame. Because the

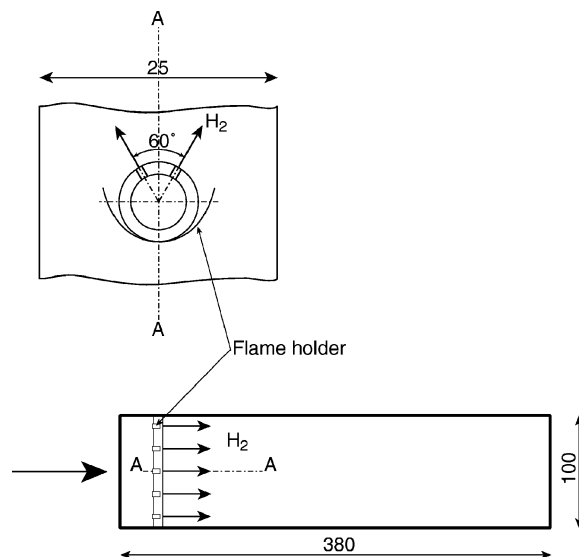


Fig. 2 Geometry of the preheater.

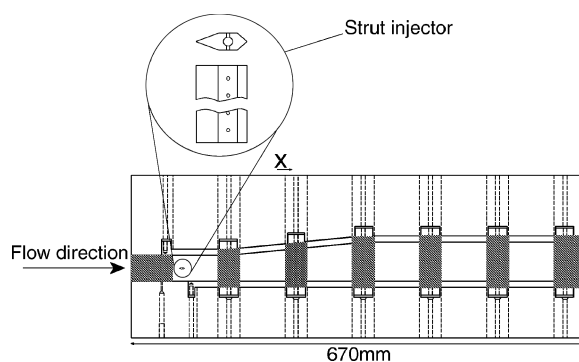


Fig. 3 Combustion chamber.

mixing process is performed also upstream in the supply tube, the preheater flame is shortened considerably, and complete burnout is obtained upstream of the entrance of the scramjet combustion chamber.

### C. Combustion Chamber

The cross-sectional area at the entrance of the combustion chamber is  $27.5 \times 25 \text{ mm}$ . At a distance of 75 mm from the inlet plane, the hydrogen fuel is injected using one of the two investigated injectors, which are described further later. The hydrogen mass flow can be varied up to  $2.3 \text{ g/s}$  by increasing the injection pressure, which is measured with an accuracy of  $\pm 2\%$ . At 145 mm downstream of the entrance, the flow in the combustion chamber is expanded continuously from 27.5 to 41.5 mm with an angle of 4 deg to prevent thermal choking.<sup>5</sup> In contrast to the modular construction of the chamber walls used in previous investigations, the experiments presented here were made with single-element walls to avoid disturbances of the flow caused by discontinuities between the modules (Fig. 3).

### D. Injectors

Two different injectors have been used in the tests. The first injector ("pylon injector") was developed by Grünig<sup>5</sup> (Fig. 4). It represents a design optimized for quick ignition and intense reaction within the combustion chamber. It consists of a massive body, which forms secondary vortices by a ramp structure at its flanks. The hydrogen is injected at an angle of 30 deg to the flow direction. Further details on this injector and the experimental results may be found in Ref. 5.

The other injector, which was designed to achieve low total pressure loss with a smaller range of flame stability (strut injector),

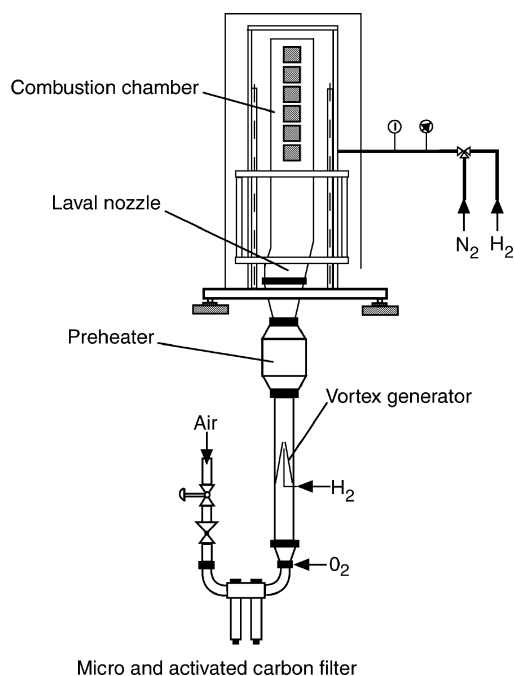


Fig. 1 Scramjet combustor and test rig.

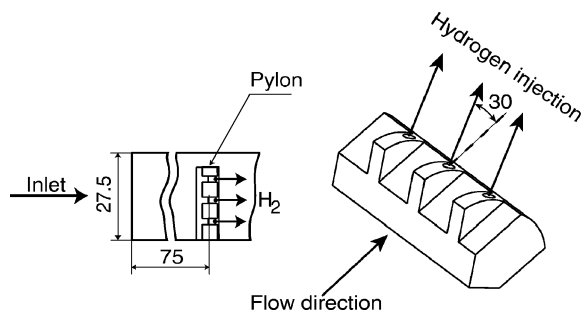


Fig. 4 Pylon injector.

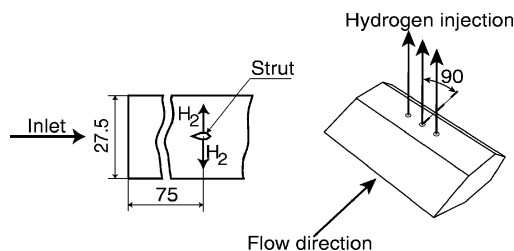


Fig. 5 Strut injector.

is shown in Fig. 5. The cross section is slender and forms a half angle of only 22.5 deg at its leading edge and a half angle of 45 deg at its trailing edge. This injector does not provide any features for the generation of secondary vortices. The fuel is injected at 90 deg to the main airstream through three orifices on each side of the strut. The orientation of the hydrogen jets relative to the airstream is shown in Figs. 4 and 5, respectively. The geometric and aerodynamic simplicity of this injector make it particularly suitable for numerical simulations using computational fluid dynamics (CFD).

### III. Investigation Tools

#### A. Shadowgraph Method

With this method, density gradients and, in particular, shocks in a supersonic flow can be visualized employing a change of the refractive index of a compressible transparent medium. The data deliver information of the flow integrated along lines of sight. In the presented investigations, a pulsed flash lamp (Nanolite) was synchronized with a charge-coupled device (CCD) camera (PCO, Flash Cam 335 CG 0045) with a resolution of  $756 \times 290$  pixel.

#### B. Rayleigh Scattering

In Rayleigh scattering, the detected signals have the same frequency as the incident laser light and are a superposition from all existing molecules in the gas mixture stimulated. Thus, this technique cannot be used for individual species concentration measurements, but it offers the possibility to visualize a flowfield with strong gradients in pressure and concentration of species with different Rayleigh cross section, for example, air and  $H_2$  (Ref. 9). The Rayleigh scattered power depends on both the total number density and the gas composition. With use of a light sheet, two-dimensional planes in the flow can be investigated, and a high spatial resolution can be obtained. A XeCl excimer laser (Lambda Physik, EMG201-204MSC) with a wavelength of 308 nm and a pulse energy of up to 400 mJ was used as light source. The elastic scattered light was detected with an intensified CCD camera (La Vision, Streak Star) and a Nikon lens (UV-Nikkor, 105 mm, 1:4.5).

#### C. OH-LIF Measurements

With the LIF, single species of interest may be detected in a gas mixture if an extremely narrow-banded light source is used for the excitation of the molecules. The detection limit of this technique is in the parts per million range. In hydrogen–air combustion, OH radicals are the only species that exist in sufficient concentrations

for LIF measurements. They can be used as marker for the start of the reaction because of their fast formation during the ignition processes. In the present measurements, a light sheet was used, which allowed the two-dimensional detection of the fluorescence signals. The molecules were excited at a wavelength of 283 nm by means of a dye laser (Lambda Physik, Scanmate 2 9703 F 2055, Coumarin 153), which was pumped by a XeCl excimer laser (Lambda Physik, EMG201-204MSC) at a wavelength of 308 nm. The corresponding energy transition was  $A^2\Sigma^+(v'=1) \leftarrow X^2\Pi(v''=0)$ . The fluorescence was detected with an intensified CCD camera (La Vision, Streak Star) and the already mentioned Nikon lens. In the experiments with the combustion chamber, the quartz windows caused reflection, which had to be suppressed by means of a bandpass mirror filter, which was adjusted to transmit at 310 nm.

#### D. Self-Fluorescence Measurements (Chemiluminescence)

The self-fluorescence technique offers the simple possibility to detect chemical reactions without using an excitation light source. In the experiments the signal was detected with an intensified CCD camera (La Vision, Streak Star) and, again, the Nikon lens. No bandpass filter was used here because the goal of the measurements was to distinguish between the different reaction types rather than to achieve a spectral selection of specific species in the reacting flow.

#### E. Numerical Simulation

All simulations were carried out with Fluent 5.5 on a Linux-cluster consisting of 32 nodes. Fluent<sup>10</sup> uses a control-volume-based technique to convert the governing equations to algebraic equations. Both structured and unstructured meshes can be used for the simulation. Fluent also allows the user to refine or coarsen the grid based on the flow solution and, thus, to improve the simulation accuracy of the shocks without enormous increase of the number of cells. The Reynolds stress model<sup>10</sup> was applied for the modeling of turbulence. The non equilibrium wall function was used for modeling the near-wall region.<sup>10</sup> The use of the near-wall modeling approach, which would be preferable for the simulation of flows with boundary-layer separation, was not possible because it requires a very fine grid resolution near the wall ( $y^+ \approx 1$ ). Such a resolution near the wall is possible only for a two-dimensional simulation because of the enormous increase of the number of cells and because of the limited computational resources. The governing equations were solved using a coupled solver with a second-order discretization scheme, which means that all values are second-order accurate.

A two-dimensional structured grid with quadrilateral cells and a three-dimensional structured grid with hexahedral cells were used for the simulation of the scramjet combustor. The average size of cells was 0.1 and 0.25 mm, and the number of cells was about 12,500 and 500,000, respectively. Additional transport equations were solved for all relevant species, and the source terms of these equations were calculated using detailed hydrogen kinetics, whereas turbulence–chemistry interaction was not considered.

Additional simulations of the flow in the Laval nozzle were carried out to obtain the profiles of the inlet parameters for the modeling of the flow in the chamber.

### IV. Results

#### A. Investigation of the Preheater

As already mentioned in the Introduction, the motivation for the current study was the discrepancy of the numerically and the experimentally obtained ignition behavior of the investigated scramjet combustor. In the simulation, the fuel did not ignite because of the short residence time in the recirculation zone of the injector, whereas in the experiment, a stable flame was obtained. Because the ignition delay is influenced tremendously by the presence of radicals, the appearance of reaction intermediates in the preheated inflow is probably the reason for the observed discrepancies. To minimize the influence of the preheater on the combustion in the scramjet test combustor, high concentrations of intermediates at the nozzle

exit must be avoided. It is highly desirable that the thermodynamic equilibrium is reached upstream of the Laval nozzle.

The kinetic analysis of the basic design of the preheater indicated that the residence time of reactive gases is long enough for complete reaction upstream of the Laval nozzle, if the assumption of perfectly stirred flow in the precombustor is made. Furthermore, the temperature in the divergent part of the Laval nozzle is low enough to recombine the radicals present after the reaction has approached thermodynamic equilibrium in the vitiator. In reality, however, perfect stirring in the combustor cannot be achieved, and the injected hydrogen burns in a diffusive flame. As a consequence, the required residence time will be longer than calculated in the kinetics study, and the available residence time in the preheater used in our tests may not be sufficient for the complete fuel–air mixing and/or for the termination of the reaction. In this case, the reaction is controlled by fuel–air mixing and not by the hydrogen kinetics.

In principle, three different effects may lead to radical concentrations above the thermodynamic equilibrium at the exit of hydrogen fuelled preheaters: 1) spatial concentration gradients in the precombustor due to low mixing intensity generated by the fuel injector or uneven fuel distribution, 2) quench of the reaction in the cold boundary layers of the vitiator and the Laval nozzle that are both water-cooled in our case, and 3) temporal fluctuation of the concentration due to insufficient small-scale mixing.

The kinetics study mentioned earlier revealed that radicals at the exit of the preheater can only exist if the probability density function<sup>11</sup> of the mixture fraction in overall lean cases is wide and the fuel richer side of the distribution approaches stoichiometric conditions. From research on lean premixed combustion in gas turbines, it is well known that achieving a temporal homogeneity is much more challenging than providing a uniform spatial fuel distribution alone. From the standpoint of kinetics modeling, temporal and spatial inhomogeneities follow the same rules, if a timescale and a combustor length scale are used.

Finding out which effect dominates in preheaters is difficult without excessive investigation of the vitiator aerodynamics. However, in the preheater used in the study, the fuel distribution tubes are well designed, the velocity of the hydrogen jets is very high compared to the velocity of the airstream, and the vitiator width is of same order as the vortices generated by the fuel injectors. For these reasons, the development of large-scale concentration gradients is not very likely. Because the LIF measurements show a homogeneous distribution of the OH radicals over the exit cross section of the Laval nozzle, there is also no indication that the observed radical emission is caused by quenching of the reaction near the water-cooled wall. As a consequence, temporal fluctuations of the equivalence ratio due to insufficient small-scale mixing is the most probable reason for the radical emission of the vitiator used in the test.

Because, according to this assumption, the burnout depends on the quality of small-scale mixing of the fuel with air, the idea of increasing the mixing time by spatial decoupling of the fuel–air mixing from the combustion zone is straightforward. In preheaters with burnout limitations due to the characteristic timescale or length scale of fuel–air mixing, premixing generally improves the burnout tremendously. For this purpose, half of the preheater fuel is injected upstream of the precombustor. Proper large-scale mixing in the air supply tube is achieved by secondary flows, which promote the large-scale distribution of the fuel and the large-scale mixing. As a consequence, the length of the combustor can now be used for improving small-scale mixing.

The application of vortex generators is an effective method for the generation of the required large-scale flow structures in the mixing tube (Fig. 6). In the selected configuration, four triangular baffle plates generate four counterrotating vortex pairs. The fuel is injected near the downstream end of the vortex generators into the flow. If the fuel is injected in the optimum angular direction, these provide the large-scale transport of the fuel and generate a uniform mixture within a few hydraulic diameters. OH-LIF measurements were carried out at the exit of the Laval nozzle for both modes at two temperature levels to assess the improvements made due to premixed

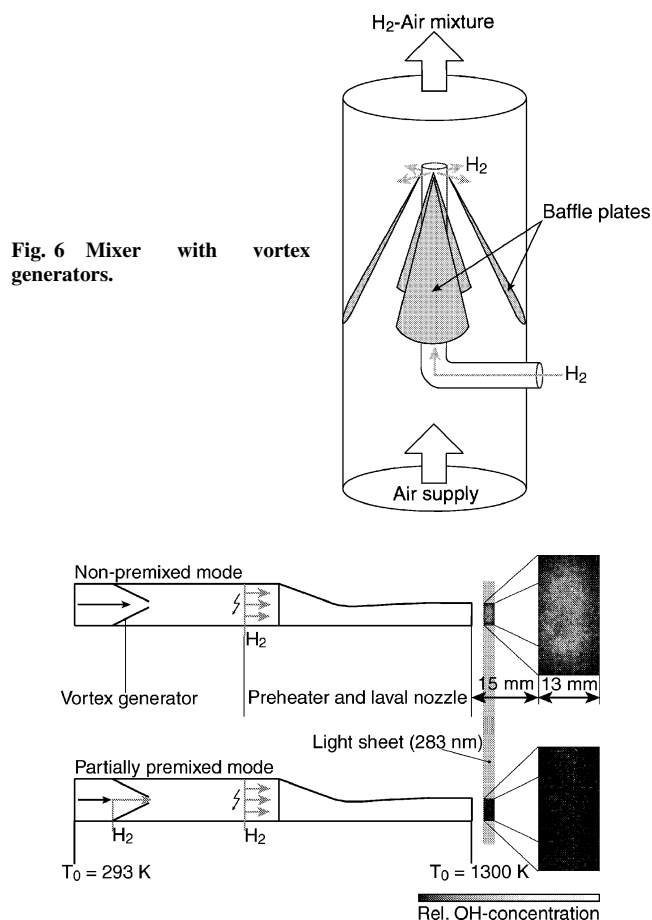


Fig. 7 OH-LIF measurements at the exit of the Laval nozzle in both preheating modes.

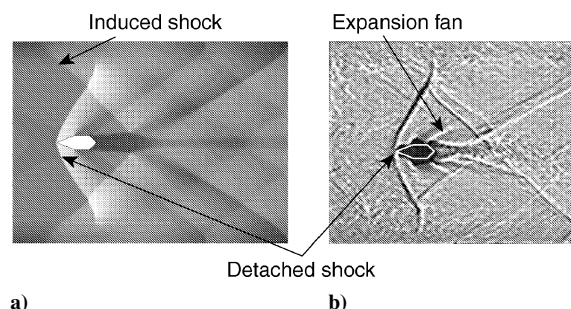


Fig. 8 Flowfield near the strut: comparison of the calculated density distribution with the shadowgraph.

combustion. The results for a total temperature of 1300 K are shown in Fig. 7.

It can be clearly seen that fluorescence signals from OH radicals far above the detection limit can be measured in the nonpremixed mode, whereas no signal was detected in partially premixed mode. The premixing of the hydrogen in the partially premixed mode improves the burnout at higher temperatures. In the nonpremixed mode, high levels of intermediates still exist at the exit of the Laval nozzle. At a temperature of 900 K, however, no signal was detected in either mode. This might be due to a shorter diffusion flame length in the vitiator or a strong recombination of the OH radicals in the Laval nozzle because of the decreasing static temperature during expansion.

## B. Investigation of the Shock System

The shocks induced by the strut injector in a cold flow without injection of hydrogen were visualized with the shadowgraph method and compared with the numerical calculation of the flow (Fig. 8).

Note that the calculated density field in the middle plane of the flow channel is displayed, whereas the shadowgraph method delivers an integrated view through the entire volume. In the center of the flow, the gas velocity is highest, and thus, the shock system produces higher density gradients there than in the wall region. For this reason, the integrated view through the flow does not differ significantly from a cut through the middle plane, and it is justified to compare the measurement with CFD results for the centerplane. The excellent consistency of the numerical and the experimental data reveals that the quality of the flow modeling on the basis of Fluent 5.5 is adequate.

Both Figs. 8a and 8b show the strong detached shock that produces a separation of the boundary layer and induces a shock wave system upstream of the separation point. The main detached shock is reflected at the boundary layer and interacts with the wake of the strut. At the trailing edge of the strut, two expansion waves are formed, and the flow direction is deflected toward the center of the channel. Another shock system is induced when the two deflected flows hit each other in the wake downstream of the strut. As a consequence, a subsonic wake with a static temperature above the self-ignition limit of hydrogen is formed.

In this two-dimensional view, one important influence of the strut on the flow cannot be visualized. At the base of the strut, shocks are induced as a result of the boundary-layer separation. To investigate its influence on the subsonic wake behind the strut, a three-dimensional CFD simulation was carried out. The subsonic area behind the strut is shown in Fig. 9. Resulting from the three-dimensional shock-boundary-layer interaction, the subsonic regions in the middle of the chamber as well as behind the strut are intensified. Obviously, the favorable high-temperature conditions in the wake of the strut promote the self-ignition of the hydrogen, if the residence time in this zone exceeds the induction period of the ignition.

### C. Hydrogen Injection

To better understand the interaction of the hydrogen jets with the airstream, Rayleigh measurements were carried out in a cold airstream with injection of hydrogen. In these experiments different planes downstream of the strut were investigated, starting from a distance  $x$  of 8–18 mm. The cold air mass flow was regulated to 300 g/s. The hydrogen mass flow was 0, 0.7, and 2.0 g/s, respectively. The orientation of the laser light sheet can be seen in Fig. 10.

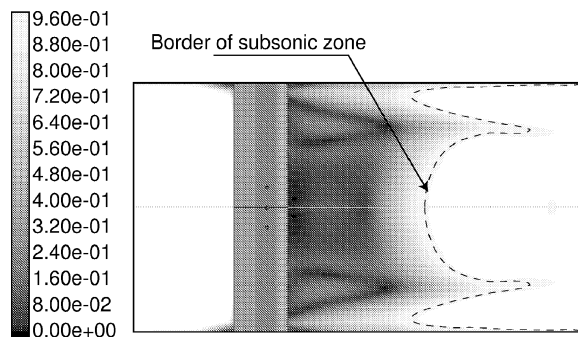


Fig. 9 Three-dimensional investigation of flowfield near the strut: Mach number distribution in the centerplane.

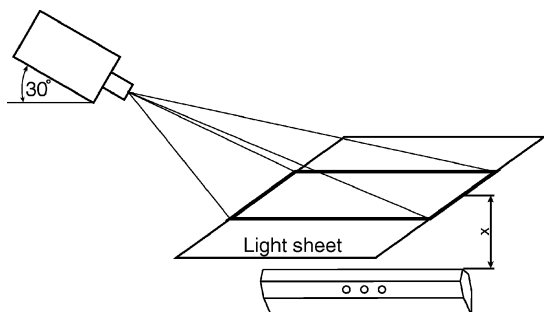


Fig. 10 Setup for Rayleigh measurements.

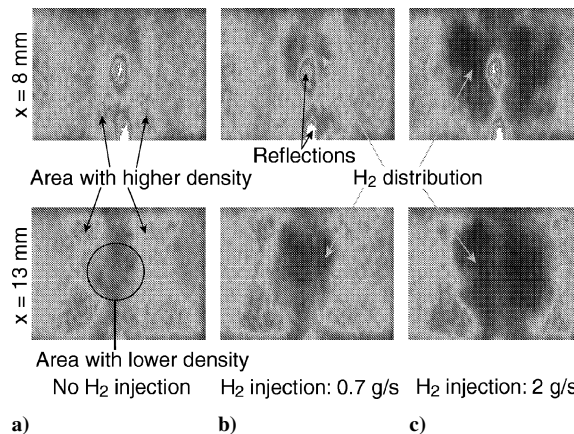


Fig. 11 Rayleigh measurements at 8 and 13 mm, downstream of the strut: a) cold airstream (300 g/s), b) cold airstream (300 g/s) with injection of 0.7 g/s hydrogen, and c) cold airstream (300 g/s) with injection of 2.0 g/s hydrogen.

The results of the measurements at the distances of 8 and 13 mm behind the trailing edge of the strut are shown in Fig. 11. Because the Rayleigh scattered power depends on both the total number density and the gas composition, the injection of hydrogen in a supersonic airstream has two different influences on the scattering signal. On one hand, the shocks in the flow cause a density gradient that leads to an increase of the molecule density behind the shock and, thus, to a stronger signal. On the other hand, hydrogen has a lower Rayleigh scattering cross section than air, and hence, the detected signal is lower in areas with a high hydrogen concentration.

The bright spots in Fig. 11 stem from the reflections of the laser light at the metal strut. The hydrogen injection starts from the center of each image and is oriented horizontally to the right and to the left side of Fig. 11. Without injection of hydrogen, the areas with higher molecule density behind the trailing edge of the strut, which show the location and structure of the shocks, are clearly visible. The side view of the corresponding shock wave system is shown in Fig. 8. Note that the shadowgraph method visualizes the change of the refractive index of a transparent medium, for example, caused by pressure gradients, whereas Rayleigh scattering displays the absolute density of a homogeneous medium. In a gas mixture, the different Rayleigh cross sections of the species dominate the intensity of the Rayleigh signal. Thus, the data from both methods cannot be compared directly.

The injection of hydrogen (0.7 g/s) influences the shock wave system considerably. This is shown in the top of Fig. 11b. The hydrogen jets induce shock curvature. Furthermore, a dark region appears that is caused by the lower Rayleigh cross section of the injected hydrogen and that illustrates the hydrogen distribution at 8 mm downstream of the trailing edge of the strut.

The top panel of Fig. 11c shows the shock structure for an injection of 2.0 g/s of hydrogen. No shock structure like in the other two cases was detected. The large dark region shows the penetration of the hydrogen jets into the airstream. The bottom panels of Fig. 11 show a plane at a distance of 13 mm downstream of the trailing edge of the strut. The operating points were the same as in the preceding case. Because the distance between the light sheet and the metal strut is greater, the light scattered at the surface is much weaker, and thus, the Rayleigh measurements are of better quality.

Figures 11a and 11b show a more similar structure of the shock wave system than before. The distribution of the hydrogen in Fig. 11b is clearly visible as a dark region. In Fig. 11c, the hydrogen jets change the flow pattern significantly compared with the other two cases. Furthermore, the hydrogen is better distributed at the high mass flow rate.

An interesting change of the density distribution can be seen in Fig. 11a: Four zones with higher density, illustrating the areas downstream of shocks, can be seen. The reason for this phenomenon is the converging shocks that are induced by the base of the strut at each side wall. They cross each other at a distance of about 15 mm

behind the trailing edge of the strut. Upstream of the crossover point of the base-induced shocks, an area with lower density exists in the center of the channel cross section. This area can be seen as a darker region in the bottom of Fig. 11a.

In summary, the injection of the hydrogen has two effects on the Mach number of the flow. The jet causes a virtual broadening of the injector and, thus, a stronger shock, which reduces the Mach number more than the injector geometry alone. This effect can be seen clearly in the top of Fig. 11b, where the shocks are bent due to injection. Furthermore, hydrogen has a sonic speed that is 3.79 times greater than that of air. This means that by the addition of hydrogen the sonic speed of the gas mixture increases and, consequently, the Mach number decreases accordingly. In Fig. 11c, the increased shock strength as well as the higher sonic speed produce a larger area with subsonic flow and flow recirculation. This effect is stronger for the higher fuel mass flow rates investigated. As a consequence of the increase of the volume of the recirculation zone, the residence time of the gas mixture in the ignition area increases.

#### D. Effects of Vitiator Performance on Ignition

Both injectors were tested with respect to their sensitivity on the radical content of the incoming air. For this purpose, the preheater was operated in nonpremixed as well as in partially premixed mode. The experiments were made with a total temperature of 1300 K and a hydrogen mass flow of 1 g/s.

The flame holding capability of the pylon injector (Fig. 4) is not influenced by the radical content of the air inflow. In both preheating modes, ignition was achieved and the flame stabilized in the wake of the pylon. These results are consistent with the results of Grünig,<sup>5</sup> who also detected flame stabilization directly in the wake of the pylon for the nonpremixed operation of the preheater.

In contrast to this observation, the flame holding capability of the strut injector (Fig. 5) depends clearly on the combustion mode in the preheater. Only in the nonpremixed mode could the flame be stabilized directly in the wake of the strut, whereas in the partially premixed mode, no reaction could be observed.

The reasons for the clear difference of the sensitivity of both injectors are the secondary vortices induced by the pylon concept that improve the mixture between fuel and air. Furthermore, the shock wave system caused by the massive pylon is much stronger than that of the slender strut injector. This leads to a higher static temperature in the flowfield downstream of the pylon. Finally, the large wake of the pylon concept provides a region where the high static temperature and the low gas speed support the ignition of the fuel. The strut injector neither produces secondary vortices nor a shock wave system of comparable strength, and the size of the wake is insufficient for the stabilization of the reaction in the partially premixed mode. For these reasons, the flame holding capabilities will be very poor during operation with clean air.

#### E. Ignition Limits of the Strut Injector

To improve the understanding concerning the influence of the operating parameters on the ignition, the strut injector was investigated in both operating modes of the preheater in greater depth. To get more detailed information about the ignition limits, the preheating temperature and injected fuel mass flow were varied. The flow was observed with the self-fluorescence technique. Three different modes could be distinguished:

- 1) In the no ignition mode, no fluorescence is observed in the combustion chamber.
- 2) In the lifted flame mode, the flame ignites detached from the strut and approached the strut with increasing total temperature and increasing fuel mass flow.
- 3) In the stabilized flame mode, the flame stabilizes in the wake of the strut.

The results of these measurements are shown in Fig. 12. A lower temperature limit for the ignition of the fuel exists in both modes at approximately 900 K. The reason for this somewhat unexpected result is the recombination of the OH radicals at the lower temperature level and was already discussed in Sec. IV.A. The recombination leads to almost identical radical concentrations for both

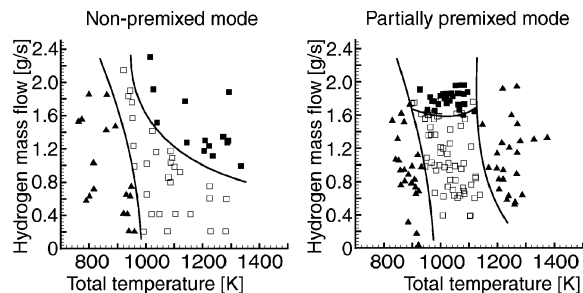


Fig. 12 Ignition and reaction in nonpremixed and partially premixed mode (strut injector): ▲, no ignition; □, lifted flame; and ■, stabilized flame.

combustion modes of the vitiator. In the temperature range from 900 to 1200 K, a lifted flame appeared that tended to approach the strut with higher preheating temperature and higher fuel mass flow. However, a flame stabilization directly in the wake of the strut could be reached only for one of the investigated fuel mass flows of 1.3 g/s in the nonpremixed mode and 1.6 g/s in the partially premixed mode, respectively. A second ignition limit above 1150 K appeared, only in the partially premixed mode, which can be explained as follows. In the investigated combustor, ignition can only occur in the wake of the strut because only there does the static temperature exceed the self-ignition temperature of hydrogen. The axial length of the recirculation zone is limited by the beginning expansion 65 mm downstream of the injector because the static temperature downstream drops below the self-ignition temperature of hydrogen. With increasing preheat, the kinetic energy of the airflow increases, and the lateral penetration of the hydrogen jets decreases. This results in a higher fuel concentration in the wake of the strut. Accordingly, the lower temperature due to the greater amount of hydrogen in the wake counteracts the increased preheating temperature, and as the consequence, the ignition delay increases. Moreover, the higher air speed has an additional direct effect on ignition because it leads to a shorter time available for the mixing of hydrogen and air. With increasing total temperature, a critical limit is reached, and the negative effect of the increased air speed on the ignition begins to overcompensate the reduction of the ignition delay time due to the temperature rise. This ignition limit is characteristic for slender injectors without additional stabilization mechanisms such as secondary vortices or strong shocks.

Interestingly, no such upper ignition limit could be observed in the nonpremixed mode. Obviously, the higher radical concentration in the flow always leads to ignition and reaction.

## V. Conclusions

A general problem of using vitiated air preheating is the potential accelerating influence of combustion intermediates on the ignition and combustion of the injected fuel. In contrast, the decelerating influence of water is moderate.

1) The sensitivity of injectors concerning the concentration of intermediates in the inflow depends on their design. Scramjet combustors with high pressure loss flame stabilizers, which provide intense flame stabilization, are insensitive to intermediates in the incoming air.

2) Well-designed scramjet combustors, which provide just as much flame stabilization as required to minimize total pressure loss, are difficult test candidates for test rigs with vitiators. Great care must be taken not to overpredict the flame holding capability available in reality.

3) For the strut geometry investigated, the critical problem is that an upper temperature ignition limit appears only in the case of full burnout in the vitiator. This phenomenon is caused by the shorter residence time of the gas mixture and the absence of flame stabilizing radicals.

At lower preheating temperatures, reaction intermediates recombine during the expansion in the Laval nozzle because of the decreasing temperature. This recombination occurs independently of

the combustion mode. Thus, the low-temperature ignition limit is not influenced by combustion intermediates.

The proper design of hydrogen fueled precombustors for the investigation of low pressure loss scramjet injectors must incorporate an analysis of the combustion process in the combustor to avoid the emission of radicals due to insufficient small-scale mixing:

1) Because the reaction in vitiators is usually mixing controlled, full burnout can be realized by improving the mixing of fuel and oxidizer. This goal can be more easily achieved by injecting fuel into the air supply than by increasing the residence time of the gas mixture or improving the flame holders in the vitiator.

2) The existence of high radical concentrations stemming from hydrogen preheating can be easily avoided, if a piloted premixed flame is generated in the vitiator.

3) Effective premixing requires the proper generation of secondary flows in the air supply tube and the proper choice of the fuel injection location and direction.

4) Because the design of a high-quality vitiator is possible with simple hardware, vitiators are an economic alternative to complex preheaters such as high-temperature electrical resistance heaters, etc.

## References

<sup>1</sup>Münzberg, H. G., *Flugantriebe*, Springer-Verlag, Berlin, 1972, Chap. 3.

<sup>2</sup>Li, J., Yu, G., Zhang, Y., Li, Y., and Qian, D., "Experimental Studies on Self-Ignition of Hydrogen/Air Supersonic Combustion," *Journal of Propulsion and Power*, Vol. 13, No. 4, 1997, pp. 538–542.

<sup>3</sup>Mitani, T., Hiraiwa, T., Sato, S., Tomioka, S., Kanda, T., and Tani, K., "Comparison of Scramjet Engine Performance in Mach 6 Vitiated and Storage-Heated Air," *Journal of Propulsion and Power*, Vol. 13, No. 5, 1997, pp. 635–642.

<sup>4</sup>Grünig, C., Avrashkov, V., and Mayinger, F., "Fuel Injection into a Supersonic Airflow by Means of Pylons," *Journal of Propulsion and Power*, Vol. 16, No. 1, 2000, pp. 29–34.

<sup>5</sup>Grünig, C., "Gemischbildung und Flammenstabilisierung bei Pyloneinblasung in Überschallbrennkammern," Ph.D. Dissertation, Dept. of Mechanical Engineering, Technical Univ. of Munich, Garching, Germany, Feb. 1999.

<sup>6</sup>Lyubar, A., and Sattelmayer, T., "Numerical Investigation of Fuel Mixing, Ignition and Flame Stabilization by a Strut Injector in a Scramjet Combustor," *Proceedings of the 11th International Conference on Methods of Aerophysical Research (ICMAR)*, Vol. 2, Nonparel Publishing House, Novosibirsk, Russia, 2002, pp. 122–127.

<sup>7</sup>Sander, T., and Sattelmayer, T., "Application of Spontaneous Raman Scattering to the Flowfield of a Scramjet Combustor," *Proceedings of the 11th International Conference on Methods of Aerophysical Research (ICMAR)*, Vol. 2, Nonparel Publishing House, Novosibirsk, Russia, 2002, pp. 143–147.

<sup>8</sup>Grünig, C., Avrashkov, V., and Mayinger, F., "Self-Ignition and Supersonic Reaction of Pylon-Injected Hydrogen Fuel," *Journal of Propulsion and Power*, Vol. 16, No. 1, 2000, pp. 35–40.

<sup>9</sup>Eckbreth, A. C., *Laser Diagnostics for Combustion Temperature and Species*, Vol. 3, Combustion Science and Technology Book Series, Gordon and Breach, 1996, Chap. 5.

<sup>10</sup>"Fluent 5.5," Documentation, Fluent, Inc., Lebanon, NH, 2000.

<sup>11</sup>Warnatz, J., Maas, U., and Dibble, R. W., *Combustion, Physical and Chemical Fundamentals, Modeling and Simulation, Experiments, Pollutant Formation*, 2nd ed., Springer, Berlin, 1999, Chap. 12.

P. Givi  
Associate Editor

## Hans von Ohain Elegance in Flight



**Margaret Conner**  
Universal Technology  
Corporation

2001, 285 pages, Hardback  
ISBN: 1-56347-520-0  
List Price: \$49.95

**AIAA Member Price: \$34.95**

This is the first book ever to chronicle the life and work of Dr. Hans von Ohain, the brilliant physicist who invented the first turbojet engine that flew on 27 August 1939. The book follows him from childhood through his education, the first turbojet development, and his work at the Heinkel Company, where his dream of "elegance in flight" was ultimately realized with the flight of the Heinkel He 178, powered by the turbojet engine he created. It also presents his immigration to the United States and his career with the United States Air Force, whereupon he became one of the top scientists in the field of advanced propulsion.

The book is a historical document, but it is also evidence of a man's dream coming true in the creation of "elegance in flight," and its impact on mankind.

### Contents:

- Hans von Ohain: a Description
- Family and Education
- Idea for a Propulsion System
- Meeting with Ernst Heinkel
- The Hydrogen Test Engine
- Other Research in Jet Propulsion
- Heinkel's Engine Developments
- First Flight of a Turbojet-Propelled Aircraft
- The Next Engine and the War
- War Planes
- Last German Efforts and Defeat
- Paperclip
- Research and the U.S. Government
- Family Life
- Aerospace Research Laboratory
- Hans von Ohain's Contributions
- Position as Chief Scientist at ARL
- Air Force AeroPropulsion Laboratory
- Work after Retirement
- Memorials
- Appendices
- Index



American Institute of Aeronautics and Astronautics

American Institute of Aeronautics and Astronautics  
Publications Customer Service, P.O. Box 960, Herndon, VA 20172-0960  
Fax: 703/661-1501 Phone: 800/682-2422 E-Mail: warehouse@aiaa.org  
Order 24 hours a day at [www.aiaa.org](http://www.aiaa.org)

02-0543